

## Phase separation, charge ordering, and pairing in layered three-dimensional systems

Yu. G. Pashkevich and A. E. Filippov

*A. A. Galkin Donetsk Phystech NASU, 83114 Donetsk, Ukraine*

(Received 22 May 2000; revised manuscript received 31 October 2000; published 2 March 2001)

The processes of Coulomb gas ordering in a three-dimensional (3D) layered system are studied by means of the Brownian dynamics approach. It is found that at different densities of the carriers, a 3D lattice of charges, as well as new specific structures, are possible in the system. At small densities, the particles inside the layers can associate into droplets that collectively repel between neighboring layers, creating 3D ordering of the droplets. These droplets possess local stripe structure that orders spontaneously along an arbitrary direction. The density of charge within the droplets is not a constant and changes with the average density. At higher densities, a specific ordering of the charges into the tetragonal-like or hexagonal-like structures is observed visually and described numerically. Specific “pairing” of the charges from neighboring layers plays an essential role in the formation of all above structures.

DOI: 10.1103/PhysRevB.63.113106

PACS number(s): 71.10.Li, 71.30.+h, 71.45.-d, 72.15.Rn

The theory of doped Mott insulators shows a variety of electronic ground states, from charge-stripe order through electronic liquid-crystal phases<sup>1,2</sup> to the usual metallic state depending on doping level. The complex character of the phase diagram is caused by the long-range Coulomb interaction between electrons placed in an antiferromagnetic background. Besides, the well-defined layered structure is a common feature of these systems. Both of these features create essential difficulties for theory. A common theoretical simplification is to solve the two-dimensional problem in different models.<sup>3-8</sup>

Here we present a three-dimensional (3D) model with very simple suppositions. We study a 3D layered crystal with Coulomb interaction among spinless charges. The particles move in a background potential that is periodic along one of the axes. It is shown that this model is sufficient to obtain density stratification (or phase separation) accompanied by classic phases such as the Wigner crystal or stripe ordering.

In particular, such a model can describe the charge ordering in systems without magnetic ions. Very likely, such a situation takes place in  $\text{Ba}_{0.6}\text{K}_{0.4}\text{BiO}_3$ . There are many hints of a remnant of charge ordering in  $\text{Ba}_{0.6}\text{K}_{0.4}\text{BiO}_3$  above the temperature of the superconducting phase transition (see, for example Ref. 9).

Let us suppose that the equally charged spinless particles move and interact in 3D space with a positive background that includes a periodic potential along one of the dimensions (which we choose as the  $z$  direction). For a sufficiently strong periodic potential, the particles should be localized in equidistant layers. For a single layer, the particles would tend to form an hexagonal (Wigner) crystal; however, this tendency can be strongly modified by the interactions between layers.

The particles from a particular layer interact with the collective potential of the surrounding layers and tend to position themselves in the potential minima. In an ideal (translationally invariant) case, the particles of one layer have to be found directly under the centers of cells of the neighboring layer. The particles from a third layer might be expected to sit directly under positions of the particles from the first one; however, the particles in the first and third layers also repel

one another. Hence, the energy minimum should be a non-trivial compromise between the interlayer and intralayer interactions.

Numerical simulations show that the symmetric positioning of the particles over the centers of the cells of the Wigner crystal is unstable. Instead, when the positions of particles in one layer are projected onto the average plane of a neighboring layer, each particle in the first layer is found to be displaced in the direction of one of the particles in the neighboring layer. In particular, the displacements break the geometric frustration in the collective position of a hexagonal 2D lattice from one layer to the next.

The situation appears as follows. Moving in the collective field of the neighboring layers, the carriers are attracted to the minima of the potential. These minima act as if they were effective “positively charged particles.” The projections of real particles from a neighboring layer (attracted to these minima) onto the  $xy$  plane can be treated as the “images” of these effective particles. In some sense this behavior is close to a stripe formation, as in the cuprates and nickelates.<sup>1,2</sup> It is directly analogous to the previously studied process of screening in a system containing two kinds of particles that bind into “pairs.” These pairs are dipolarly charged and form, in their turn, chains of dipoles.<sup>10</sup>

Let us note that the “pairs” are formed by particles from different layers. So, this pairing is essentially a 3D phenomenon. We found that the variation of the density leads to other nontrivial structures, also. In particular, at low density, the system produces an unusual “droplet phase.” This phase consists of the charged droplets with an internal structure. It is possible that the specific dipolar chain structure or structuralized droplet phase might have relevance to the problem of the mechanism of superconductivity in novel superconductors.

To study the structures appearing in the system of moving charges placed into 3D compensating background, with periodically modulated potential along one of the dimensions, we apply the Brownian dynamics (BD) technique. This technique has been widely applied in recent years<sup>11,12</sup> (in particular, by one of the present authors<sup>13,14</sup>) to simulate the behavior of various systems.

The technique is based on the solution of the system of dynamic equations for the particles with discrete coordinates  $\mathbf{R}_j = (x_j, y_j, z_j)$ , where  $1 \leq j \leq N$ , and the vectors  $\mathbf{R}_{jk} = \mathbf{R}_j - \mathbf{R}_k = (x_j - x_k, y_j - y_k, z_j - z_k)$  connecting pairs of particles. The choice of appropriate boundary conditions depends on the specific problem.

The equations in such an approach contain some random noise sources.<sup>12–14</sup> Together with relaxation terms, these simulate the effect of finite (nonzero) temperature (in accordance with the well-known fluctuation-dissipation theorem). Spatially continuous densities are determined *a posteriori* by means of a summation over realizations and averaging over a sufficiently long time. The necessary length of time for averaging is determined numerically for each problem.<sup>13,14</sup>

In particular, the particle density in real space,  $\varrho(\mathbf{R}) = [\langle \sum_j \delta(\mathbf{R} - \mathbf{R}_j) \rangle]_{t_0}$ , is obtained by a summation  $\sum_j$  over particle coordinates and averaging  $[\langle \dots \rangle]_{t_0}$  over characteristic time  $t_0$ . This density is used to calculate the correlation functions of the problem (for example: the two-point correlation function  $G(\mathbf{R}, \mathbf{R}') = \langle \varrho(\mathbf{R}) \varrho(\mathbf{R}') \rangle$ , where  $\langle \dots \rangle$  denotes an averaging over an ensemble of particles). The set of the correlation functions gives complete information about the thermodynamic properties of the system.

The set of BD equations can be written in the form

$$\ddot{\mathbf{R}}_j + \gamma \dot{\mathbf{R}}_j + \frac{\partial}{\partial \mathbf{R}_j} V(\mathbf{R}_j) + \frac{\partial}{\partial \mathbf{R}_j} \sum_k U(\mathbf{R}_{jk}) = \delta F(\mathbf{R}_j; t),$$

where  $\gamma$  is a relaxation constant. To model a thermal bath, we apply the Gaussian random force  $\delta F(t)$ ,

$$\langle \delta F(\mathbf{R}; t) \rangle = 0;$$

$$\langle \delta F(\mathbf{R}; t) \delta F(\mathbf{R}'; t') \rangle = 2\gamma T \delta(\mathbf{R} - \mathbf{R}') \delta(t - t')$$

The periodic one-particle potential is chosen to have the form  $V(\mathbf{R}_j) = V_0 \cos(2\pi k \cdot z_j / L_z)$

The system is supposed to be continued periodically. Here  $L_z/k$  is the period of the potential along the  $z$  axis, with  $k$  an integer. Along the other two axes the system is quasi-infinite. The boundary conditions along all of the axes lead to the interaction of each particle with all other particles inside the calculation volume  $\Omega = L_x \cdot L_y \cdot L_z$ , as well as with all of their “images” obtained as a result of the translation of particle coordinates across (beyond) the nearest boundary.<sup>12–14</sup> So, the many-body potential  $U(\mathbf{R}_{jk})$  in the equations contains the vectors  $x_{jk} = x_j \pm L_x, y_{jk} = y_j \pm L_y, z_{jk} = z_j \pm L_z$  with all possible permutations. The sign “+” or “-” is determined by a direction to the nearest boundary plane along given axis.

If a particle leaves the volume  $\Omega = L_x \cdot L_y \cdot L_z$  along one of the axes it is returned to the volume. In the absence of an external field, the particle return can be done by means of mirror reflection, or by cyclic shift. In the second case, the corresponding projection of the velocity is conserved, and the coordinate projection is shifted as follows:  $x_j \rightarrow x_j \pm L_x, y_j \rightarrow y_j \pm L_y, z_j \rightarrow z_j \pm L_z$ .<sup>13</sup>

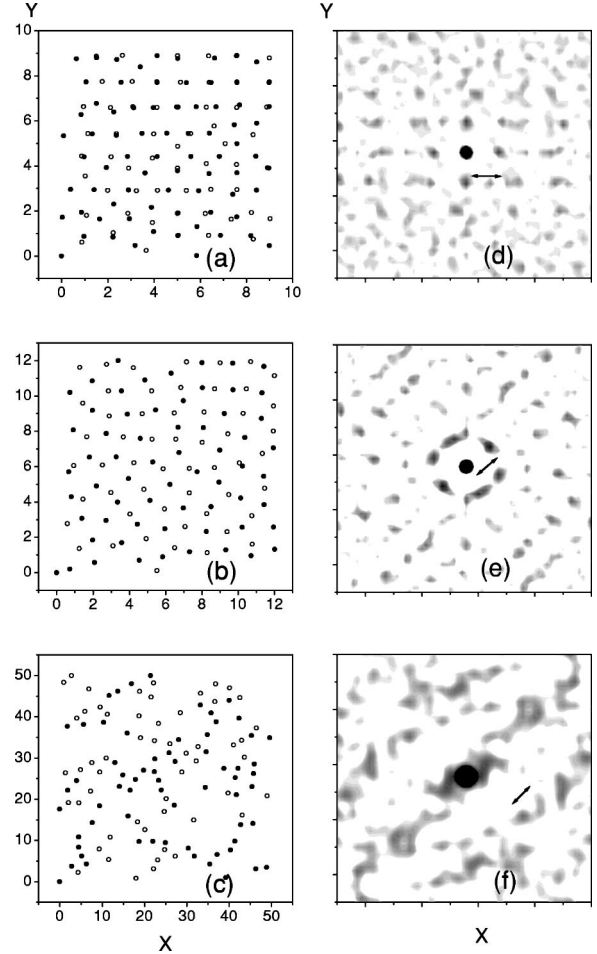


FIG. 1. Instantaneous configurations of the particles at the final stage of evolution are shown for the three characteristic densities: (a) at  $L=9$ ; (b) at  $L=12$ ; (c) at  $L=50$  ( $N=256$ ). The projections of the particles from neighboring layers are shown by black and white circles, respectively. Two-point correlation function  $G(\mathbf{R} - \mathbf{R}') = \langle \varrho(\mathbf{R}) \varrho(\mathbf{R}') \rangle$  is presented for following three typical cases: (d) well-pronounced tetragonal lattice (at  $L=7$ ); (e) for hexagonal ordering of the particles inside the layers ( $L=10.5$ ); (f) for droplet phase with an internal stripe structure appearing at phase separation (at small density  $L=50$ ). The length of arrows indicate the value of the averaged minimal distance between particles.

The many-body potential  $U(\mathbf{R}_{jk}) = U_c \cdot U_{scr}$  consists of a long-range Coulomb interaction  $U_c(\mathbf{R}_{jk}) \propto 1/|\mathbf{R}_{jk}|$  with a screening factor  $U_{scr}(\mathbf{R}_{jk}) \propto \exp(-|\mathbf{R}_{jk}|/r_0)$ .

Numerical results for the case  $L_x = L_y = L, L_z = 5, T = 1, \gamma = 3$ , and  $r_0 = 10^3$  are summarized in Figs. 1–3. For definiteness, all instantaneous configurations shown were obtained in the frames of uniform motion. Random distributions of the charges have been taken as the initial conditions, which is the standard choice used in a search for an energy minimum by the relaxation technique and by simulated annealing.<sup>7</sup>

The same fixed number of particles,  $N=256$ , has been used in all cases. The charge density is varied by changing the cross section  $L_x \cdot L_y$  of the calculation volume  $\Omega = L_x \cdot L_y \cdot L_z$ . To check for finite-size effects, the calculations

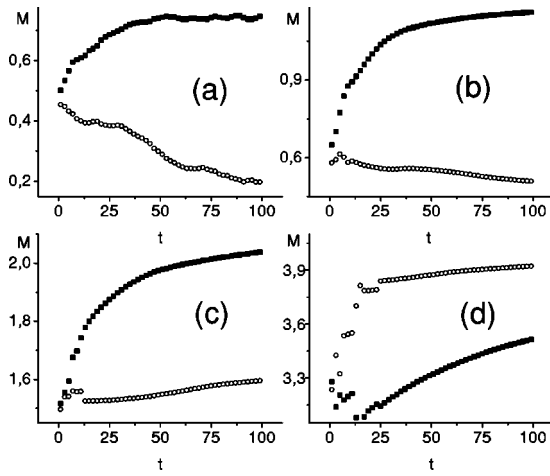


FIG. 2. Time dependence of averaged minimal distance between the projections of particles from the same layer (black circles) and nearest layers (white circles): (a) at  $L=9$ ; (b)  $L=10.5$ ; (c) at  $L=11$ ; (d) at  $L=70$  ( $N=256$ ).

were reproduced at some densities for other numbers of particles ( $N=128$  and  $N=512$ , with a respectively chosen cross section of the box  $L_x \cdot L_y$ ).

Instantaneous particle configurations at the final (but not equilibrium) stages of structure formation are shown in Figs. 1(a)–1(c) for three specific densities. The particle coordinates for two adjacent layers are shown by means of different symbols in a projection onto the  $xy$  plane (all other particles are not shown). The case (a) corresponds to high density ( $L=9$ ). The configuration (b) corresponds at long time to a density close to a critical value ( $L=12$ ). At small density ( $L=50$ ) a kind of clusterization into “droplets” occurs in the system. These droplets contain segments of charge chains and, therefore, possess some kind of fine structure. The droplets from different layers repulse mutually. The state obtained looks similar to the concentration stratification (or

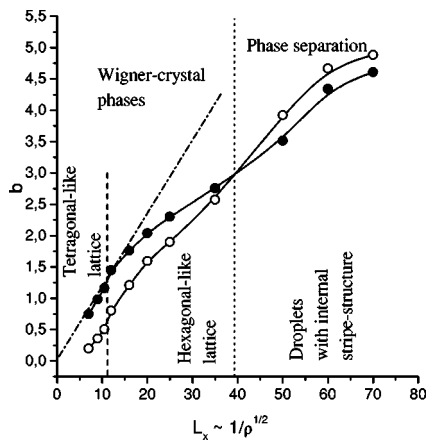


FIG. 3. A dependence of equilibrium averaged minimal distance between the particles  $b = \langle \min\{|\mathbf{R}_{jk}|\} \rangle$  from density (shown as a function from box size  $L$  at a fixed number of particles  $N=256$ ). Two kinds of circles denote the values of  $b$  corresponding to the particles from the same layers (black circles) or different layers (white circles).

phase separation) found in a system with two kinds of particles.<sup>10</sup> For brevity we will use “phase separation” to describe our droplet state.

In the initial stage of the evolution, the particles spontaneously group to the vicinities of the planes corresponding to the minima of the periodic potential  $V(\mathbf{R}_j) = V_0 \cos(2\pi k \cdot z_j/L_z)$ . These minima define the “layers.” For definiteness, we denote a particle as belonging to a given layer if its  $z$  coordinate differs from that of the layer by no more than 0.1 of distance between the layers, i.e.,  $|z - z_k| < 0.1|z_{k+1} - z_k|$ . It is interesting to note that typical for this stage is a tendency to “pairing” (in projection onto the  $xy$  plane) of the particles from neighboring layers.

Below, this tendency will be characterized numerically. Such a state survives for the majority of particles only for some high densities. A tetragonal 3D structure is found to be natural for this case in the final equilibrium state. Nevertheless, a remnant pairing plays an important role in the formation of the droplet phase at low densities.

One can use the time dependence of the averaged minimal distance between particles  $b = \langle \min\{|\mathbf{R}_{jk}|\} \rangle$  as a numerical characteristic to distinguish different scenarios that occur as a function of density  $\rho$ . This value corresponds to the mean distance between nearest neighbors. Different mutual relations and a sign of inequality between values of  $b$  inside a layer and for pairs of neighboring layers reflects a difference between visually observed structures.

Four qualitatively different scenarios of evolution of the distance between nearest particles are shown in Fig. 2; (a) high density ( $L=9$ ); (b) a density close, but slightly higher, than a critical one ( $L=10.5$ ); (c) a density close to, but lower than, the critical one ( $L=11$ ); and finally (d) a very low density ( $L=70$ ). The averaged projections of the distances within a layer and between layers are indicated by black and white circles, respectively.

For a fixed distance between the layers, the average interaction between the layers is proportional to the density. When the density is high enough, this interaction is strong enough to order particles in a 3D structure. Figure 1(d) presents the correlation function of a typical tetragonal crystal structure that is obtained at high density ( $L=7$ ). However, long wavelength  $z$  displacements of the particles inside each of the layers caused by strong interactions along the  $z$  axis prevent the formation of an ideal 3D tetragonal lattice.

When the density goes through the critical value ( $10.5 < L < 11$ ), the force binding of the particles in the layers prevails over the  $z$  component of the interaction between layers. The particles are locked strongly in the layers and ordered hexagonally. Naturally, the mean distance between nearest neighbors stabilizes with time. However, the distance between the projections of particles from different layers does not tend to zero now (as it does for the 3D tetragonal lattice). This fact is reflected by the difference in behavior of the lower lines in Figs. 2(a)–2(c).

Finally, when the density is extremely low, the repulsion between the particles from different layers is notable for sufficiently big groups of particles. Phase separation occurs

now. The particles combine into clusters (or droplets). The projections of the clusters from different layers mutually fill in free spaces for each other.

All these structures are reflected by the correlation function  $G(\mathbf{R}, \mathbf{R}') = \langle \varrho(\mathbf{R}) \varrho(\mathbf{R}') \rangle$  shown in Figs. 1(d)–1(f). The function  $G(\mathbf{R}, \mathbf{R}') = \langle \varrho(\mathbf{R}) \varrho(\mathbf{R}') \rangle$  is calculated for a single layer and shown for the following three typical cases: (d) a well-pronounced tetragonal lattice (at  $L=7$ ); (e) hexagonal ordering ( $L=10.5$ ); (f) droplet phase appearing at phase separation into charge-rich and charge-poor domains (at small density  $L=50$ ). The filament structure formed by the scraps of charge chains is visible. In all figures the averaged minimal distance between particles within a layer is marked by the arrows.

These results have been checked for different (rectangular) forms of the boundary. A tendency to form stripes or chains of charge along one of the spontaneously chosen direction is observed in all cases. As is seen, for instance, in Fig. 1(c), the local direction of the stripes does not depend on the boundary orientation. The stripes form local groups (domains) with common but arbitrary orientation, so, the local structure is not an artifact of the system boundaries. However, the numerically found global structure correlates with the periodic boundaries. The difference between the local and global orientations is reflected by the correlation function shown in Fig. 1(f).

The dependence of the equilibrium averaged minimal distance between the particles  $b$  on density is summarized in Fig. 3. As before, two kinds of circles denote the values of  $b$  corresponding to particles from the same or different layers.

The slopping dash-dotted line gives the slope of the  $b(L)$  function for the ideal tetragonal lattice.

This plot can be treated as a phase diagram in terms of the mean density  $\varrho \propto 1/L_x L_y$  at fixed  $L_z$ . The vertical dashed line (at  $L \approx 11$ ) denotes a transition between two different structures. Just to the right of the line, the ratio of the in-plane to interplanar distance passes through  $\sqrt{3}$ , whose relation corresponds to ideal 3D hexagonal ordering.

The dotted vertical line corresponds to a transition from a charge-order-like Wigner crystal to the phase-separation structure that contains charge-rich droplets with an internal fine structure. It should be noted that the curves  $b(L)$  do not reach horizontal asymptote.

To conclude, we found a transition from a Wigner crystal phase to a droplet phase with an internal structure. The density of the charges inside the droplets depends on the value of mean density in the system. In spite of some analogy with liquid droplets, this result occurs in the absence of a direct attraction among the particles. The particles in an insulating layer cannot collect in compact droplets; rather, the particles close to the droplet boundaries essentially attract between different layers. As a result, the size of the droplets is always comparable with the distance between them. From a physical point of view, the dependence of the internal density of charge in the droplets as a function of the doping level is one of the most important features of this new droplet phase.

We appreciate discussions with J. Tranquada. This work is supported in part by the INTAS Grant No 96-0410 and SFRR research Grant No. 2.4/199 of Ukraine.

<sup>1</sup>S.A. Kivelson, E. Fradkin, and V.J. Emery, *Nature (London)* **393**, 550 (1998); V.J. Emery, S.A. Kivelson, and J.M. Tranquada, *cond-mat/9907228* (unpublished).

<sup>2</sup>J. Zaanen, *J. Phys. Chem. Solids* **59**, 1769 (1998), and references therein.

<sup>3</sup>V.J. Emery and S.A. Kivelson, *Physica C* **209**, 597 (1993).

<sup>4</sup>E. Dagotto, *Rev. Mod. Phys.* **66**, 763 (1994); E. Dagotto, *J. Phys. Chem. Solids* **59**, 1699 (1998), and references therein.

<sup>5</sup>S.R. White and D.J. Scalapino, *Phys. Rev. Lett.* **80**, 1272 (1998); **81**, 3227 (1998).

<sup>6</sup>P. C. Hammel, B. J. Suh, J. L. Sarrao, and Z. Fisk, *cond-mat/9809096*, and references therein (unpublished).

<sup>7</sup>B.P. Stojkovic, Z.G. Yu, A.R. Bishop, A.H. Castro Neto, and N. Gronbech-Jensen, *Phys. Rev. Lett.* **82**, 4679 (1999).

<sup>8</sup>M. Veilette, Ya.B. Bazaliy, A.J. Berlinskii, and C. Kallin, *Phys. Rev. Lett.* **83**, 2413 (1999).

<sup>9</sup>Y. Yacoby, S.M. Heald, and E.A. Stern, *Solid State Commun.* **101**, 801 (1997).

<sup>10</sup>A.E. Filippov, *Zh. Éksp. Teor. Fiz.* **112**, 1739 (1997) [*Sov. Phys. JETP* **85**, 949 (1997)].

<sup>11</sup>M.G. Rozman, M. Urbakh, and J. Klafter, *Phys. Rev. Lett.* **77**, 683 (1996).

<sup>12</sup>O.M. Braun, A.R. Bishop, and J. Roder, *Phys. Rev. Lett.* **79**, 3692 (1997).

<sup>13</sup>O.M. Braun, B. Hu, A. Filippov, and A. Zeltser, *Phys. Rev. E* **58**, 1311 (1998).

<sup>14</sup>E.V. Vakarin, A.E. Filippov, and J.P. Badiali, *Phys. Rev. Lett.* **81**, 3904 (1998).